curves revealed a 2-year overall survival rate of 65.3%. The mean survival time for recurrent carcinomas was 22.8 months. Patients treated for primary carcinoma had a mean survival time of 34.5 months. Of the 5 patients with primary head and neck cancer, 4 (80%) were alive and without evidence of disease 2 years after treatment. The acute and chronic adverse side effects were manageable. No relevant complications concerning tissue transfer were observed. Schiefke *et al.* [48] concluded that surgical resection combined with HDR-ISBT can lead to long-term remission, and that simultaneous microvascular defect reconstruction provides tissue cover for brachytherapy.

Bartochowska *et al.* reported the results of HDR- and PDR-ISBT in the palliative treatment of patients with locally or regionally recurrent head and neck cancers [49]. PDR- and HDR-ISBT were used in 106 and 50 patients, respectively, from January 2002 to November 2008. In 8 patients, brachytherapy procedures were performed in combination with simultaneous chemotherapy (details were not shown). Sixteen patients were additionally treated with interstitial hyperthermia. All patients were regularly followed up within 6 months of final treatment. Local control, complication, and survival rates were assessed. Complete remission and partial remission 6 months after final treatment were achieved in 37.7% of patients, whereas survival rates 12 and 24 months after brachytherapy were 40% and 17%, respectively. The overall complication rate was 35%. The results of the study by Bartochowska *et al.* [49] suggest that HDR- and PDR-ISBT are safe alternatives in the palliative treatment of patients with locally or regionally recurrent head and neck cancers with relapse in a previously irradiated area who were not qualified for, or rejected surgery. These treatments offer a good palliative effect with acceptable complication rates.

DISCUSSION

The oral cavity is essential in coordinating the complex functions of deglutition, phonation and airway protection. Preserving its function is a difficult challenge when treating carcinoma in this anatomical region. The treatment modalities available include surgery, EBRT, brachytherapy and various combinations of the three. The wide range of results in the literature leaves considerable uncertainty as to the treatment of choice, but years of experience in the treatment of head and neck tumors with radiotherapy has demonstrated that a high tumor dose is required to achieve local control.

Sresty *et al.* reported that the ISBT treatment modality produces equal or superior planning results when compared with intensity-modulated radiation therapy (IMRT) [50]. Fifteen patients with tongue cancer treated with HDR-ISBT were replanned. Tongue cancer was evaluated using the IMRT planning system. Contouring of target volume, including all critical structures, was done using the IMRT treatment planning system to closely match the implant brachytherapy planning system. Prescription goals were specified and treatment plans generated. The conformity index and doses to critical organs were then calculated and compared between IMRT and ISBT. Planning time was also recorded for both the techniques in all the cases. Very good dose conformity was observed in ISBT, similar to that observed in IMRT. Dose to critical structures was lower in ISBT in all cases. Planning time was also less in ISBT for many cases. These results encouraged the authors to continue ISBT [50]. They concluded that ISBT is an ideal solution for high-dose delivery exclusively to the primary tumor volume, while limiting the risks of severe xerostomia or trismus [1, 3, 6].

HDR hyperfractionated ISBT has the following advantages: (i) accurate calculations made possible by complete fixation of the guide tubes, (ii) parallel source arrangement with the sophisticated technique, (iii) homogeneous dose distribution due to stepping source optimization, (iv) better patient care in normal wards with elimination of radiation exposure to medical staff, administration on an outpatient basis in several cases, and (v) shorter treatment times than with EBRT. Future uses of HDR-ISBT include the introduction of a 3D image-based approach for GTV and CTV assessment. Development is in progress of a common language to describe the concepts and define the terms to be used in this promising field [1].

HDR-ISBT treatment should be executed carefully, because the short treatment times allow no time for correction of errors that could result in harm to patients. Hence all personnel involved in HDR brachytherapy must be well trained and constantly alert during treatment delivery [28]. The development of well-controlled randomized trials addressing issues of efficacy, toxicity, quality of life, and costs-versus-benefits will ultimately define the role of HDR brachytherapy [28].

One of the limitations of HDR-ISBT is a lack of experience. For example, studies examining prognostic factors in LDR-ISBT allowed improvement of the technique. Treatment now involves leaded protection of the mandible, optimal intersource spacing (1.2–1.4 cm), calculations of volume treated (30 cm^3, i.e. three loops), accurate safety margins (5 mm), and effective dose rates (0.5 Gy/h). The total dose [65 Gy in brachytherapy alone, 25 Gy in combination with EBRT (50 Gy) in primary carcinomas of the oral cavity, 60 Gy in recurrent cancer in previously irradiated tissues] and an optimal interval between EBRT and brachytherapy (<20 days) have also been determined for LDR-ISBT [1, 3, 6]. Those factors remain to be established for HDR-ISBT.

PDR-ISBT appeared to be functionally equivalent to continuous ISBT. The results of PDR-ISBT should improve with better dose rate control and optimization of the dose

distribution [51, 52]. Brenner *et al.* reported the superiority of daytime PDR-ISBT over continuous LDR-ISBT [51]. However, if PDR-ISBT is applied with curative intent, the treatment unit is unavailable for treatment of other patients. As HDR-ISBT remote-controlled after-loading units are not available at all institutions, and many patients require treatment with the units that are available, continuous LDR-ISBT and daytime PDR-ISBT are difficult to perform for patients with head and neck cancer.

Due to the paucity of evidence in the literature, and the fact that few institutions are equipped to test the potential of HDR-ISBT for the convenience of patients and medical staff, the future of HDR-ISBT is uncertain. However, many studies conclude that this therapeutic mode should be explored further. In summary, although more concrete evidence is warranted, HDR-ISBT may be an important option for treatment of oral cancer.

ACKNOWLEDGEMENTS

The authors are deeply appreciative of Prof. Teruki Teshima, Prof. Toshihiko Inoue (Inoue To) and Prof. Takehiro Inoue (Inoue Ta) for their wonderful leadership throughout these studies.

REFERENCES

1. Mazeron JJ, Ardiet JM, Haie-Méder C *et al.* GEC-ESTRO recommendations for brachytherapy for head and neck squamous cell carcinomas. *Radiother Oncol* 2009;**91**:150–6.
2. Paine CH, Ash DV. Interstitial brachytherapy: past-present-future. *Int J Radiat Oncol Biol Phys* 1991;**21**:1479–83.
3. Erickson BA, Demanes DJ, Ibbott GS *et al.* American Society for Radiation Oncology (ASTRO) and American College of Radiology (ACR) practice guideline for the performance of high-dose-rate brachytherapy. *Int J Radiat Oncol Biol Phys* 2011;**79**:641–9.
4. Guedea F, Venselaar J, Hoskin P *et al.* Patterns of care for brachytherapy in Europe: updated results. *Radiother Oncol* 2010;**97**:514–20.
5. Petera J, Matula P, Paluska P *et al.* High dose rate versus LDR brachytherapy in the treatment of tongue carcinoma - a radiobiological study. *Neoplasma* 2009;**56**:163–8.
6. Nag S, Cano ER, Demanes *et al.* The American Brachytherapy Society recommendations for high-dose-rate brachytherapy for head-and-neck carcinoma. *Int J Radiat Oncol Biol Phys* 2001;**50**:1190–8.
7. Lau H, Hay J, Flores A *et al.* Seven fractions of twice daily high dose-rate brachytherapy for node-negative carcinoma of the mobile tongue results in loss of therapeutic ratio. *Radiother Oncol* 1996;**39**:15–8.
8. Leung TW, Wong VY, Wong CM *et al.* High dose rate brachytherapy for carcinoma of the oral tongue. *Int J Radiat Oncol Biol Phys* 1997;**39**:1113–20.
9. Leung TW, Wong VY, Kwan KH *et al.* High dose rate brachytherapy for early stage oral tongue cancer. *Head Neck* 2002;**24**:274–81.
10. Ohga S, Uehara S, Miyoshi M *et al.* High-dose-rate brachytherapy with local injection of bleomycin for N0 oral tongue cancer – possibilities of the control of tumor implant by inserting applicators and the decrease in tumor dose. *Nihon Igaku Hoshasen Gakkai Zasshi* 2003;**63**:47–50 (in Japanese).
11. Umeda M, Komatsubara H, Ojima Y *et al.* A comparison of brachytherapy and surgery for the treatment of stage I-II squamous cell carcinoma of the tongue. *Int J Oral Maxillofac Surg* 2005;**34**:739–44.
12. Nishioka T, Homma A, Furuta Y *et al.* A novel approach to advanced carcinoma of the tongue: cases successfully treated with combination of superselective intra-arterial chemotherapy and external/high-dose-rate interstitial radiotherapy. *Jpn J Clin Oncol* 2006;**36**:822–6.
13. Patra NB, Goswami J, Basu S *et al.* Outcomes of high dose rate interstitial boost brachytherapy after external beam radiation therapy in head and neck cancer – an Indian (single institutional) learning experience. *Brachytherapy* 2009;**8**:248–54.
14. Guinot JL, Santos M, Tortajada MI *et al.* Efficacy of high-dose-rate interstitial brachytherapy in patients with oral tongue carcinoma. *Brachytherapy* 2010;**9**:227–34.
15. Shigematsu Y, Masaki N, Ikeda H *et al.* Current status and future of brachytherapy. *Gan No Rinsho* 1983;**29**:695–701 (in Japanese).
16. Inoue To, Inoue Ta, Teshima T. High dose rate interstitial brachytherapy for mobile tongue cancer: part 1. Phase I/II study of HDR hyperfractionated interstitial brachytherapy for oral cancer. *Jpn J Cancer Chemother* 2000;**27** Suppl II:287–90.
17. Orton CG, Seyedsadr M, Somnay A. Comparison of high and LDR remote afterloading for cervix cancer and the importance of fractionation. *Int J Radiat Oncol Biol Phys* 1991;**21**:1425–34.
18. Teshima T, Inoue T, Ikeda H *et al.* Phase I/II study of high-dose rate interstitial radiotherapy for head and neck cancer. *Strahlenther Onkol* 1992;**168**:617–21.
19. Sasaki S, Teshima T, Murayama S *et al.* Comparison of radiation mucositis after interstitial brachytherapy between LDR and HDR. *Head and Neck Cancer* 1993;**19**:197–200.
20. Yoshioka Y, Yoshida K, Shimizutani K *et al.* Proposal of a new grading system for evaluation of tongue hemiatrophy as a late effect of brachytherapy for oral tongue cancer. *Radiother Oncol* 2001;**61**:87–92.
21. Inoue T, Inoue T, Yoshida K *et al.* Phase III trial of high vs. LDR interstitial radiotherapy for mobile tongue cancer. *Int J Radiat Oncol Biol Phys* 2001;**51**:171–5.
22. Yamazaki H, Inoue T, Yoshida K *et al.* Brachytherapy for early oral tongue cancer: LDR to high dose rate. *J Radiat Res* 2003;**44**:37–40.
23. Yamazaki H, Inoue T, Yoshida K *et al.* Comparison of three major radioactive sources for brachytherapy used in the treatment of node negative T1-T3 oral tongue cancer: influence of age on outcome. *Anticancer Res* 2007;**27**:491–497.
24. Kakimoto N, Inoue T, Inoue T *et al.* Results of low- and high-dose-rate interstitial brachytherapy for T3 mobile tongue cancer. *Radiother Oncol* 2003;**68**:123–8.

25. Akiyama H, Yoshida K, Shimizutani K *et al.* Dose reduction trial from 60 Gy in 10 fractions to 54 Gy in 9 fractions schedule in high-dose-rate interstitial brachytherapy for early oral tongue cancer. *J Radiat Res* 2012;**53**:722–6.
26. Mochizuki S, Kanehira C, Sekine H *et al.* A study on optimum time-dose relationship in high dose rate interstitial radiotherapy. *Jpn J Clin Radiol* 1994;**39**:1151–4.
27. Yoshida K, Nose T, Koizumi M *et al.* The usefulness of metal markers for CTV-based dose prescription in high-dose-rate interstitial brachytherapy. *J Jpn Soc Ther Radiol Oncol* 2002; **13**:253–60.
28. Nag S. High dose rate brachytherapy: its clinical applications and treatment guidelines. *Technol Cancer Res Treat* 2004;**3**:269–87.
29. Yoshida K, Yamazaki H, Takenaka T *et al.* A dose-volume analysis of magnetic resonance imaging-aided high-dose-rate image-based interstitial brachytherapy for uterine cervical cancer. *Int J Radiat Oncol Biol Phys* 2010;**77**:765–72.
30. Mikami M, Yoshida K, Takenaka T *et al.* Daily computed tomography measurement of needle applicator displacement during high-dose-rate interstitial brachytherapy for previously untreated uterine cervical cancer. *Brachytherapy* 2011;**10**:318–24.
31. Donath D, Vuong T, Shenouda G *et al.* The potential uses of high-dose-rate brachytherapy in patients with head and neck cancer. *Eur Arch Otorhinolaryngol* 1995;**252**:321–4.
32. Rudoltz MS, Perkins RS, Luthmann RW *et al.* High-dose-rate brachytherapy for primary carcinomas of the oral cavity and oropharynx. *Laryngoscope* 1999;**109**:1967–73.
33. Inoue Ta, Inoue To, Yamazaki H *et al.* High dose rate versus LDR interstitial radiotherapy for carcinoma of the floor of mouth. *Int J Radiat Oncol Biol Phys* 1998;**41**:53–8.
34. Guinot JL, Arribas L, Chust ML *et al.* Lip cancer treatment with high dose rate brachytherapy. *Radiother Oncol* 2003;**69**:113–5.
35. Kotsuma T, Yoshida K, Yoshida M *et al.* Brachytherapy for buccal cancer: evaluation of HDR-ISBT. 2008;**20**:s141.
36. Nishimura Y, Yoshihiko Yokoe Y *et al.* High-dose-rate brachytherapy using molds for oral cavity cancer: The technique and its limitations. *Int J Clin Oncol* 1998;**3**:351–6.
37. Ariji E, Hayashi N, Kimura Y *et al.* Customized mold brachytherapy for oral carcinomas through use of high-dose-rate remote afterloading apparatus. *Oral Surg Oral Med Oral Pathol Oral Radiol Endod* 1999;**87**:508–12.
38. Obinata K, Ohmori K, Shirato H *et al.* Experience of high-dose-rate brachytherapy for head and neck cancer treated by a customized intraoral mold technique. *Radiat Med* 2007;**25**:181–6.
39. Kudoh T, Ikushima H, Kudoh KT *et al.* High-dose-rate brachytherapy for patients with maxillary gingival carcinoma using a novel customized intraoral mold technique. *Oral Surg Oral Med Oral Pathol Oral Radiol Endod* 2010;**109**:e102–8.
40. Chatani M, Tsuboi K, Yagi M *et al.* High dose rate brachytherapy using molds after chemoradiotherapy for oral cavity cancer. *Jpn J Radiol* 2012;**30**:40–4.
41. Matsuzaki H, Takemoto M, Hara M *et al.* Two-piece customized mold technique for high-dose-rate brachytherapy on cancers of the buccal mucosa and lip. *Oral Surg Oral Med Oral Pathol Oral Radiol Endod* 2012;**113**:118–25.
42. Glatzel M, Büntzel J, Schröder D *et al.* High-dose-rate brachytherapy in the treatment of recurrent and residual head and neck cancer. *Laryngoscope* 2002;**112**:1366–71.
43. Martínez-Monge R, Gómez-Iturriaga A, Cambeiro M *et al.* Phase I-II trial of perioperative high-dose-rate brachytherapy in oral cavity and oropharyngeal cancer. *Brachytherapy* 2009;**8**:26–33.
44. Do L, Puthawala A, Syed N: Interstitial brachytherapy as boost for locally advanced T4 head and neck cancer. *Brachytherapy* 2009;**8**:385–91.
45. Krüll A, Friedrich RE, Schwarz R *et al.* Interstitial high dose rate brachytherapy in locally progressive or recurrent head and neck cancer. *Anticancer Res* 1999;**19**:2695–7.
46. Hepel JT, Syed AM, Puthawala A *et al.* Salvage high-dose-rate (HDR) brachytherapy for recurrent head-and-neck cancer. *Int J Radiat Oncol Biol Phys* 2005;**62**:1444–50.
47. Narayana A, Cohen GN, Zaider M *et al.* High-dose-rate interstitial brachytherapy in recurrent and previously irradiated head and neck cancers – preliminary results. *Brachytherapy* 2007;**6**:157–63.
48. Schiefke F, Hildebrandt G, Pohlmann S *et al.* Combination of surgical resection and HDR-brachytherapy in patients with recurrent or advanced head and neck carcinomas. *J Craniomaxillofac Surg* 2008;**36**:285–92.
49. Bartochowska A, Wierzbicka M, Skowronek J *et al.* High-dose-rate and pulsed-dose-rate brachytherapy in palliative treatment of head and neck cancers. *Brachytherapy* 2012;**11**:37–43.
50. Sresty NV, Ramanjappa T, Raju AK *et al.* Acquisition of equal or better planning results with interstitial brachytherapy when compared with intensity-modulated radiotherapy in tongue cancers. *Brachytherapy* 2010;**9**:235–8.
51. Brenner DJ, Schiff PB, Huang Y *et al.* Pulsed-dose-rate brachytherapy: design of convenient (daytime-only) schedules. *Int J Radiat Oncol Biol Phys* 1997;**39**:809–15.
52. Strnad V, Melzner W, Geiger M *et al.* Role of interstitial PDR brachytherapy in the treatment of oral and oropharyngeal cancer. A single-institute experience of 236 patients. *Strahlenther Onkol* 2005;**181**:762–7.

J. Radiat. Res., 53, 154–158 (2012)

Technical Report

Interstitial Brachytherapy Using Virtual Planning and Doppler Transrectal Ultrasonography Guidance for Internal Iliac Lymph Node Metastasis

Ken YOSHIDA[1,2*], Mari UEDA[3], Hideya YAMAZAKI[4], Tadashi TAKENAKA[3], Mineo YOSHIDA[1], Shunsuke MIYAKE[3], Susumu YOSHIDA[5], Masahiko KOIZUMI[6,7], Chiaki BAN[8] and Eiichi TANAKA[1]

Virtual planning/Doppler transrectal ultrasonography/Interstitial brachytherapy/Internal iliac lymph node.

To expand the indications for high-dose-rate interstitial brachytherapy (HDR-ISBT) for deep-seated pelvic tumors, we investigated the usefulness of Doppler transrectal ultrasonography (TRUS) guidance and virtual planning. The patient was a 36-year-old female. She had right internal iliac lymph node oligometastasis of vaginal cancer 12 months after radical radiotherapy. The tumor could not be found by gray-scale TRUS and physical examination. Virtual planning was performed using computed tomography with template and vaginal cylinder insertion. We uploaded the images to our treatment planning software and reconstructed the contours of the clinical target volume (CTV) and right internal iliac vessel. Virtual needle applicators were plotted using the template holes for virtual planning. At the time of implantation, Doppler TRUS was used to prevent vessel injury by needle applicators. Applicators were implanted in accordance with virtual planning and Doppler TRUS could detect the right iliac vessel. The percentage of CTV covered by the prescribed dose was 99.8%. The minimum dose received by the maximally irradiated 0.1-cc volume for the right internal iliac vessel was 95% prescribed dose. Complete response was achieved, however, radiological findings showed marginal recurrence at 15 months after HDR-ISBT. Post-radiation neuropathy occurred as a late complication four months after treatment; however, the pain was well controlled by medication. We consider that virtual planning and Doppler TRUS are effective methods in cases where it is difficult to detect the tumor by physical examination and gray-scale TRUS, thereby expanding the indications for ISBT.

INTRODUCTION

Interstitial brachytherapy (ISBT) for pelvic malignancy is a useful method with potential for use as a curative treatment modality. However, deep-seated tumors such as those in internal iliac lymph nodes are not good candidates for ISBT because of the difficultly in inspecting and palpating such tumors. Recently, transrectal ultrasonography (TRUS) has been incorporated into ISBT, thereby enabling us to treat deep-seated tumors.[1–4] However, it is sometimes difficult to visualize deep-seated tumors by TRUS because bowel contents may degrade the image quality.

We present a case report in which these obstacles were overcome. First, Doppler TRUS could detect the tumor at implantation when the tumor could not be visualized via gray-scale TRUS before implantation. Then, virtual planning enabled us to identify the relationship between the tumor locations and implantation points in template holes. These devices assisted in precise implantation of needle applicators without any major complications.

*Corresponding author: Phone: +81-6-6942-1331,
Fax: +81-6-6943-6467,
E-mail: kyoshida@onh.go.jp

[1]Department of Radiation Oncology, National Hospital Organization Osaka National Hospital, 2-1-14, Hoenzaka, Chuo-ku, Osaka-city, 540-0006, Japan; [2]Institute for Clinical Research, National Hospital Organization Osaka National Hospital; [3]Department of Radiology, National Hospital Organization Osaka National Hospital; [4]Department of Radiology, Kyoto Prefectural University of Medicine; [5]Department of Obstetrics and Gynecology, Kaizuka City Hospital; [6]Department of Radiology, Kaizuka City Hospital; [7]Division of Medical Physics, Oncology Center, Osaka University Hospital; [8]Department of Obstetrics and Gynecology, National Hospital Organization Osaka National Hospital.

doi:10.1269/jrr.11142

MATERIALS AND METHODS

Patient characteristics

The patient was 36-year-old female. She had a vaginal cancer categorized as cT3N1M0 using UICC classification of 2009. The right internal iliac lymph node was swollen. A biopsy of the primary lesion was performed and histological findings confirmed squamous cell carcinoma. She received combined external beam radiotherapy (EBRT) and high-dose-rate (HDR) ISBT with concurrent chemotherapy (nedaplatin) from January to February 2009. EBRT was performed at Kaizuka City Hospital and the treatment doses were 30 Gy in 15 fractions for the whole pelvis, 20 Gy in 10 fractions for center-shielded EBRT, and 10 Gy in 5 fractions for right internal iliac lymph node metastasis. HDR-ISBT was administered to the primary site (30 Gy in 5 fractions).

The primary tumor was controlled until this point; however, the right internal iliac lymph node metastasis showed regrowth 12 months after the first treatment. She complained of right hip and leg pain. The recurrent node had a maximum diameter of 16 mm and positron emission tomography (PET) showed positive uptake. The tumor marker (SCC) value was elevated to 1.6 despite the nadir value being 0.8 after the first therapy.

Virtual planning

Preplanning was performed after template insertion with a vaginal cylinder. We used a modified acryl template used for the prostate (Taisei medical, Osaka, Japan), with a custom-made vaginal cylinder and button stopper (Fig. 1). Because cylinder is positioned in a direction perpendicular to the template, applicators could be implanted parallel to the template holes.

We obtained computed tomography (CT) images and uploaded these images to our treatment planning software (Oncentra® Brachy; Nucletron B.V., Veenendaal, The Netherlands). We reconstructed the contours of the gross tumor volume as the clinical target volume (CTV), the vessel near the tumor as the organ at risk, and the pelvic bone (Fig. 2a). We also obtained the contour of the template and vaginal cylinder.

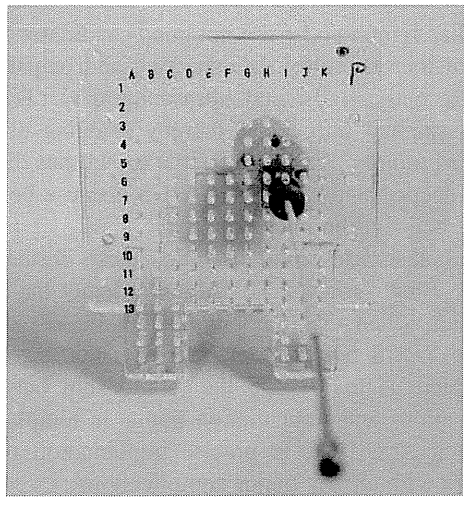

Fig. 1. Template and vaginal cylinder. We used an acryl template (Taisei medical, Osaka, Japan), used for the prostate. The vaginal cylinder (light blue) was made of silicone and fixed to the template by a red button.

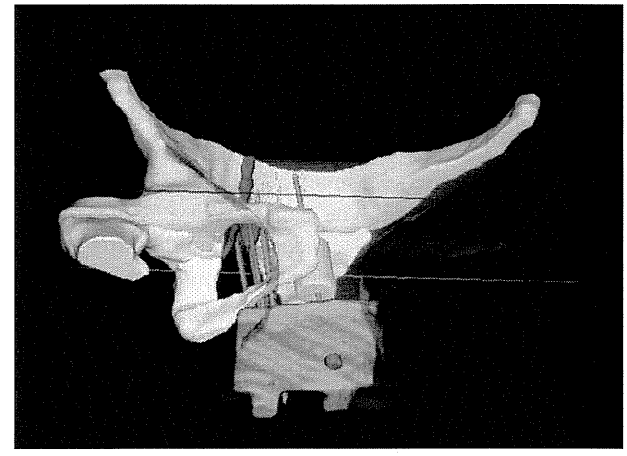

Fig. 2a. CT images uploaded to the treatment planning software. The contours of the gross tumor volume as clinical target volume (purple), right internal iliac vessel (red) as organ at risk, and pelvic bone (white) are reconstructed from the CT images. The contour of the template (green) and vaginal cylinder (light blue) is also reconstructed. Virtual applicators are also plotted (blue).

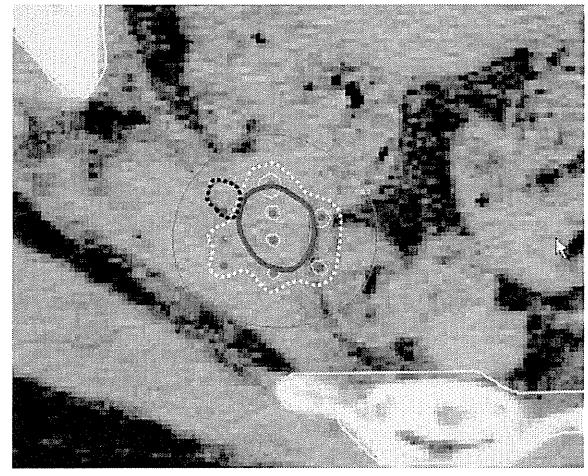

Fig. 2b. Virtual dose distribution curve. Fifty to 200% prescribed doses are shown (blue solid line = 50%, white dotted line = 100%, orange solid line = 150%, and white solid line = 200%). The clinical target volume (red) could be covered by the isodose curve of the prescribed doses (white dotted line) without excessive doses to the right internal iliac vessel (black dotted line).

Next, we plotted template holes as applicator points on both edges of the perineal skin side (cranial side) and the opposite side (caudal side). After plotting, Oncentra® Brachy indicated the applicator points by showing the expected coordinates of these points. Using this function, we plotted the virtual applicator points in the patient's body. We selected the most suitable template holes for implantation and plotted each of the apex points of the applicators as if they were actual implantation points.

Finally, we performed treatment planning. We selected adequate dwell positions and plotted an isodose curve to deliver the prescribed doses for CTV without excessive doses to the vessel near the tumor (Fig. 2b).

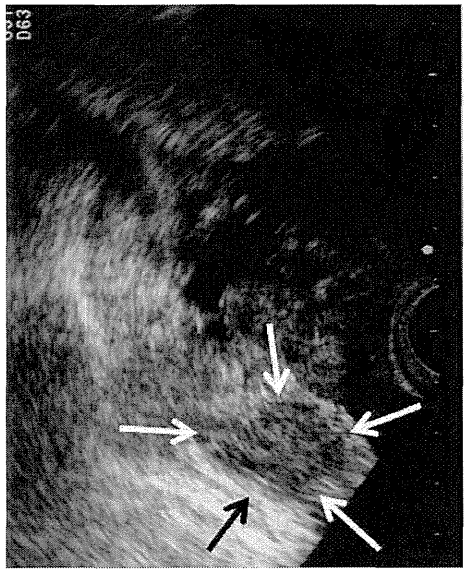

Fig. 3a. Transrectal ultrasonography showing the tumor lesion as a low echoic area (arrows).

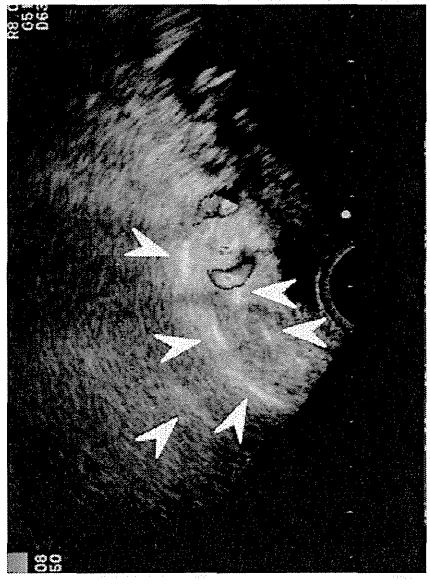

Fig. 3b. Transrectal ultrasonography showing the applicators into or around the tumor as high echoic areas (arrow heads). The color Doppler function shows two vessel flows near the tumor.

Applicator implantation

Applicator implantation was performed in the operating

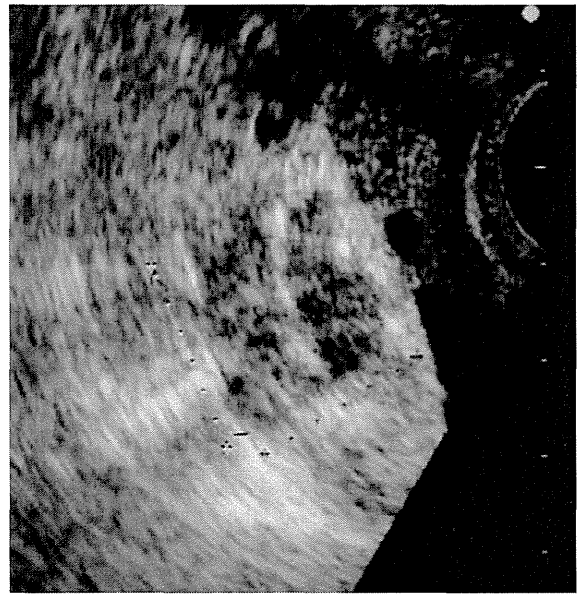

Fig. 3c. Transrectal ultrasonography after implantation. A three-plane implant was performed.

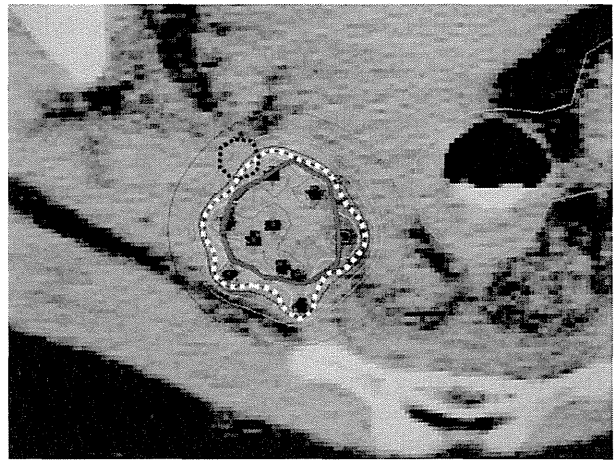

Fig. 4. Actual dose distribution curve. Fifty to 200% prescribed doses are shown (outer green solid line = 50%, outer yellow solid line = 70%, light blue solid line = 80%, blue solid line = 90%, white dotted line = 100%, white solid line = 120%, pink solid line = 130%, inner green solid line = 150%, and inner yellow solid line = 200%). The clinical target volume (red line) is well covered by the isodose curve of the prescribed doses. The minimum dose received by the maximally irradiated 0.1-cc volume and the maximum dose for the right internal iliac vessel (black dotted line) was 5.7 Gy and 7.3 Gy, respectively.

room under lumbar and continuous epidural anesthesia. The implantation was monitored by TRUS with a color Doppler function (Prosound α-7®; ALOKA Co. Ltd., Tokyo, Japan). We inserted the template–cylinder complex the same way as for preplanning.

First, we carefully implanted a flexible needle applicator (ProGuide Sharp Needle®; Nucletron B.V., Veenendaal, The Netherlands). We monitored the applicator point by TRUS. We moved the TRUS probe cranially and monitored the expected applicator position before the actual applicator tip reached the position to prevent large vessel injury. Large vessels were clearly observed using the color Doppler function. We also monitored the expected applicator implantation point to acquire the tumor image. At the calculated depth from the perineal skin where the applicator would reach the tumor lesion, we found a low echoic area (Fig. 3a). We also visualized the vessel near the tumor using the color Doppler function. This finding seemed consistent with the CT/magnetic resonance imaging (MRI) findings before implantation, and hence, we surmised that the low echoic area must be a recurrent tumor.

Next, we pushed the applicator deeply and stopped when we felt hard resistance; the length of the inserted applicator at this time was the same as the distance between the perineal skin and pelvic bone measured at the time of virtual planning. On the basis of these findings, we were convinced that our virtual planning was very effective in terms of a successful first needle applicator implantation. Using the same procedure, we implanted a total of 10 applicators with color Doppler guidance (Fig. 3b, c).

After implantation, we extracted the template–cylinder complex and only the applicators were rested on the patient's perineal skin. For treatment planning, CT and MRI were performed. CT-based planning was performed using MRI as a reference to contour CTV. The CTV was delineated with the assistance of axial T2-weighted MR images. We determined dwell positions of the treatment source to cover the CTV and used an additional 15-mm cranial margin for needle displacement except when the applicator tip was stopped by the pelvic bone before an extra implantation of 15 mm.

Treatment planning was performed using the PLATO® planning system (version 14.2; Nucletron B.V., Veenendaal, The Netherlands) and Oncentra® Brachy with manual modification.[5] We used microSelectron-HDR® (Nucletron B.V., Veenendaal, The Netherlands) with an ^{192}Ir source for treatment.

RESULTS AND DISCUSSION

CT and MRI revealed that the applicators displaced slightly laterally compared with virtual planning. However, we could deliver the prescribed doses to CTV after computer optimization with manual modification (Fig. 4). The right internal iliac vessel near CTV could not be visualized by CT; however, MRI could detect the vessel and was useful for planning (Fig. 5). We administered 48 Gy in 8 fractions as the prescribed dose, in accordance with our protocol.[6] The percentage of CTV covered by the prescribed dose (V100) was 99.8%. The minimum dose received by the maximally irradiated 0.1-cc volume and the maximum dose for the right internal iliac vessel was 5.7 Gy (95% prescribed dose) and 7.3 Gy (122% prescribed dose), respectively.

Treatment was completed without any difficulty. The patient complained of additional perineal and right lower leg pain because of the implant. This pain was controlled by epidural anesthesia and non-steroidal anti-inflammatory drug. After treatment was completed, the pain was reduced; however the pain caused by the tumor and/or implant continued.

The tumor marker value decreased from 1.6 to 0.6 at three months after ISBT. PET showed complete response at 11 months after ISBT. However, radiological findings showed marginal recurrence at 15 months after ISBT. Post-radiation neuropathy occurred as a late complication four months after treatment and the patient of complained of increased right leg pain. She was admitted for pain control and was prescribed fentanyl (2.1 mg; Durotep® Patch).

Deep-seated pelvic tumors are a challenge for adequate implantation, even with image guidance. Although TRUS is often used for gynecological ISBT,[1–4] it was rarely indicated for deep-seated pelvic tumors like the present case. Usually implantation is performed in centrally located regions such as the uterus, vagina, or cervical stump, and pelvic sidewall and lymph node lesions are not suitable for implantation. One of the reasons for this is because detecting tumor lesions by TRUS and physical examination is difficult, especially in the case of lymph node metastasis.[7,8]

Heneghan JP *et al.* demonstrated that color flow imaging and pulsed Doppler imaging provide additional useful infor-

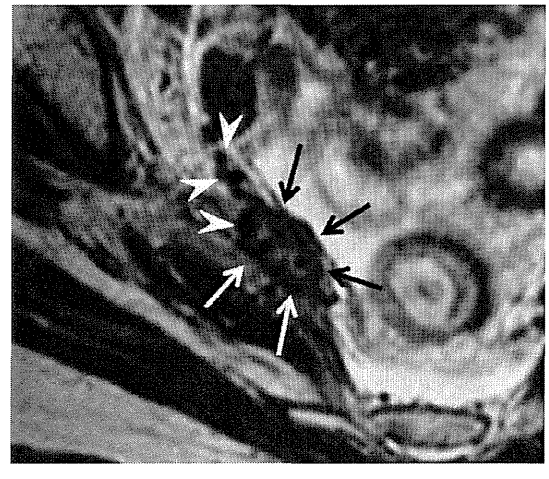

Fig. 5. MRI after implantation. The tumor lesion (arrows) and vessel (arrow heads) are visualized clearly. Applicators are visualized as low intensity dots.

mation to gray-scale TRUS in staging primary rectal cancer.[9] However, there are few reports for gynecological cancer. We have applied Doppler TRUS, which clearly visualized the vessel near the tumor. Doppler TRUS was very useful not only for detecting the tumor but also for avoiding vessel injury by virtue of precise implantation guidance. We consider that Doppler TRUS guidance has potential for use in ISBT, especially for tumors near large vessels.

Another important aspect in the treatment of our patient was virtual planning. Virtual planning for pelvic tumors has been reported by Eisburch *et al.*[10] who used custom-made plastic templates attached to the perineum through which a cylindrical plastic vaginal obturator was inserted. They then loaded the entire set of CT images into the treatment planning system. CTV, organs at risk, and the vaginal cylinder were contoured on each axial CT slice and displayed as three-dimensional structures. The authors provided a "cylinder's eye view," which is the view of the anatomy as seen from the external end of the vaginal cylinder looking down the long axis of the cylinder. The implantation points were decided on the basis of the cylinder's eye view. Because applicators were implanted parallel to the cylinder, cylinder's eye view is very useful for the physician to select adequate implantation points. They decided the optimal angles for unimpeded view of the tumor and adequate needle depth to cover the tumor. They achieved a good local control rate (55%).

However, there is a shortcoming in this report of Eisburch *et al.* They did not perform MRI. We performed MRI-assisted image-based treatment for previously gynecological ISBT.[11] Because of the usage of a removable template, we could achieve MRI-assisted image-based treatment and it will leads to good treatment conformity. The dose–volume histogram findings were satisfactory. V100 was 99.8% and the CTV was almost covered by the prescribed doses. However, unfortunately, marginal recurrence was occurred at 15 months after ISBT. No consensus was achieved about the dose–volume relationship for the organs at risk, especially, in the case of reirradiation. This aspect will be deliberated upon in further studies.

We consider that virtual planning and Doppler TRUS have a possibility to become an effective method in cases where it is difficult to detect the tumor by physical examination and gray-scale TRUS, thereby expanding the indications for ISBT.

ACKNOWLEDGEMENT

This study was supported in part by the Ministry of Education, Culture, Sports, Science and Technology (Grant-in-Aid for Young Scientists (A) 21689034). We would like to thank Yukiko Tokuda, M.D., Kazuya Honda R.T.T., Yasushi Yoshimura R.T.T., Kazumasa Aramoto, R.T.T. and the other staff of the Departments of Radiology, Obstetrics and Gynecology, Anesthesiology and Nursing staff for helping us in many ways during the completion of this paper.

REFERENCES

1. Weitmann HD, *et al* (2006) Ultrasound-guided interstitial brachytherapy in the treatment of advanced vaginal recurrences from cervical and endometrial carcinoma. Strahlenther Onkol **182**: 86–95.
2. Stock RG, *et al* (1997) A new technique for performing Syed-Neblett template interstitial implants for gynecologic malignancies using transrectal-ultrasound guidance. Int J Radiat Oncol Biol Phys **37**: 819–825.
3. Erickson B, *et al* (1995) Ultrasound-guided transperineal interstitial implantation of pelvic malignancies: Description of the technique. Endocuriether Hyperthermia Oncol **11**: 107–113.
4. Sharma DN, *et al* (2010) Use of transrectal ultrasound for high dose rate interstitial brachytherapy for patients of carcinoma of uterine cervix J Gynecol Oncol **21**: 12–17.
5. Yoshida K, *et al* (2002) The usefulness of metal markers for CTV-based dose prescription in high-dose-rate interstitial brachytherapy. J Jpn Soc Ther Radiol Oncol **13**: 253–260.
6. Kotsuma T, *et al* (2011) Preliminary results of magnetic resonance imaging-aided high-dose-rate interstitial brachytherapy for recurrent uterine carcinoma after curative surgery. J Radiat Res **52**: 329–334.
7. Marano P, *et al* (1993) Experience with the combined diagnosis and therapy of locally advanced carcinoma of the uterine cervix (stage FIGO IIB-III). Transrectal ultrasonography and CT in the staging and in follow-up after therapy. Preliminary results. Radiol Med **86**: 630–638.
8. Fischerová D, *et al* (2009) Use of transrectal ultrasound and magnetic resonance imaging in the staging of early-stage cervical cancer. Ceska Gynekol **74**: 323–329.
9. Heneghan JP, *et al* (1997) Transrectal sonography in staging rectal carcinoma: the role of gray-scale, color-flow, and Doppler imaging analysis. Am J Roentgenol **169**: 1247–1252.
10. Eisbruch A, *et al* (1998) Customized gynecologic interstitial implants: CT-based planning, dose evaluation, and optimization aided by laparotomy. Int J Radiat Oncol Biol Phys **40**: 1087–1093.
11. Yoshida K, *et al* (2010) A dose-volume analysis of magnetic resonance imaging-aided high-dose rate image-based interstitial brachytherapy for uterine cervical cancer. Int J Radiat Oncol Biol Phys **77**: 765–772.

Received on August 4, 2011
Accepted on October 5, 2011
J-STAGE Advance Publication Date: January 13, 2012

ANTICANCER RESEARCH *32*: 4467-4472 (2012)

Diffusion-weighted MRI and PSA Correlations in Patients with Prostate Cancer Treated with Radiation and Hormonal Therapy

YUKO IRAHA[1], SADAYUKI MURAYAMA[1], AYANO KAMIYA[1], SHIRO IRAHA[2] and KAZUHIKO OGAWA[3]

[1]*Department of Radiology, Graduate School of Medical Science, University of the Ryukyus, Okinawa, Japan;*
[2]*Department of Radiology, Okinawa South Medical Center, Okinawa, Japan;*
[3]*Department of Radiation Oncology, Osaka University Graduate School of Medicine, Osaka, Japan*

Abstract. *Aim: To investigate the correlation between signal intensity (SI) on diffusion-weighted imaging (DWI) and the levels of prostate-specific antigen (PSA) in patients with prostate cancer treated with radiation and hormonal therapy. Patients and Methods: Forty-four patients with prostate cancer treated with hormonal therapy and radiation therapy were evaluated. Areas with high SI on DWI were detected and the apparent diffusion co-efficient (ADC) values were measured. The ADC values and PSA levels were compared between patients with high-DWI SI and patients with a normal DWI signal. Results: Fourteen patients had high SI on DWI. The mean ADC value in these cancerous lesions was lower than in non-cancerous tissues. The mean PSA level in patients with high-DWI SI was significantly higher than in patients with a normal signal. Conclusion: The present results suggest that SI on DWI appears to correlate with PSA levels in patients with prostate cancer treated with radiation and hormonal therapy.*

Prostate-specific antigen (PSA) is widely used for screening, diagnosis, determination of prognosis, selection of appropriate treatment, and for predicting disease status after treatment of prostate cancer in men (1).

Magnetic resonance imaging (MRI) is now a major imaging modality for prostate cancer detection and localization. MRI techniques have recently progressed, and can provide good quality diffusion-weighted images (DWI), especially with the use of parallel imaging techniques. DWI can be used to detect malignant tumours. Several investigators have reported on the potential usefulness of DWI for detecting prostate cancer that is in part due to the lower apparent diffusion co-efficient (ADC) values of tumor compared to the non-cancerous regions of the prostate (2-6). DWI may also provide qualitative and quantitative information for measuring therapeutic response in patients with prostate cancer during and after radiotherapy. On the contrary, imaging methods have not been widely used in daily practice to assess the effect of hormonal therapy or disease status after hormonal therapy in patients with prostate cancer. Furthermore, few investigations have reported on the usefulness of DWI for assessment of the radiation and hormonal therapy response for prostate cancer (7-10).

In the present study, the performance of DWI for visualizing prostate cancer treated with radiation and hormonal therapy was investigated, and the correlation between the signal intensity (SI) on DWI and the PSA levels was examined.

Correspondence to: Yuko Iraha, Department of Radiology, Graduate School of Medical science, University of the Ryukyus, 207 Uehara, Nishihara-cho, Okinawa, 903-0215, Japan. Tel: +81 988951162, Fax: +81 988951420, e-mail: irayu@med.u-ryukyu.ac.jp

Key Words: Prostate cancer, hormonal therapy, radiation therapy, diffusion-weighted MRI, prostate-specific antigen.

Patients and Methods

Patients. This study was approved by our Institutional Review Board. Written informed consent was waived because of the retrospective nature of the analysis. Between May 2007 and April 2010, 44 patients with biopsy-proven prostate cancer underwent hormonal therapy prior to radiation therapy, and underwent MRI examinations before and after radiation therapy. The median patient age was 72 years (range=55-81 years). The median Gleason score was 7 (range=5-9). The mean PSA level before all therapy was 31.4 ng/ml (range=5-270 ng/ml). Nineteen of the men were at high risk, 17 were at intermediate risk, and eight were at low risk according to the classification by D'Amico *et al.* (11). The mean PSA level after the start of hormonal therapy and before radiation therapy was 0.66 ng/ml (range=0.01-10.31 ng/ml). Table I presents the patients' characteristics. The median interval from prostate biopsy to MRI examination was 7.5 months (range=0.5-96.1 months). The median interval from the start of hormonal therapy to the start of radiation therapy was 6.4 months (range=0.2-83.6 months). All MRI were carried out before radiation therapy and 3 to 4 months after the completion of therapy.

0250-7005/2012 $2.00+.40

All patients received hormonal therapy with a luteinizing hormone releasing-hormone analog and an anti-androgen. Radiation therapy was administered at 2 Gy/fraction to a total dose of 72-76 Gy (mean dose=75.4 Gy) with the use of 10-MV modulated radiation therapy.

MRI techniques. All images were collected using a 1.5-T MRI system (Intera Achieva; Philips Healthcare, Best, the Netherlands), equipped with a five-channel phased-array coil. All patients underwent DWI in addition to imaging studies using a routine prostate MRI protocol. Axial T1- and T2-weighted images and coronal T2-weighted images with spectral pre-saturation with inversion recovery (SPIR) were acquired.

Imaging parameters for T1-weighted imaging were as follows: repetition time/echo time (TR/TE)=497/12 ms, echo-train length (ETL)=5, bandwidth (BW)=217.7 kHz, field of view (FOV)=22 cm, slice thickness/gap=4/1 mm, number of excitations (NEX)=4, matrix size=288×288, and sensitivity-encoding (SENSE) factor=2. The time required to acquire the T1-weighted image set was 2 minutes and 47 seconds.

Imaging parameters for turbo spin-echo T2-weighted imaging were as follows: TR/TE=4700/120 ms, ETL=11, BW= 145.9 kHz, FOV=22 cm, slice thickness/gap=4/1 mm, NEX=4, matrix size=288×288, and SENSE factor=2. The time required to acquire the T2-weighted image set was 2 minutes and 44 seconds.

Axial echo-planar DWI with STIR was performed using slice locations similar to those used for T1- and T2-weighted image sequences, respectively, using the following parameters: b values=0, 800 and 2,000 s/mm2, TR/TE=6000/80 ms, TI=160-170 ms, BW=41.4 kHz, FOV=25 cm, slice thickness/gap=4/0.6 mm, NEX=3, matrix size=80×80, and SENSE factor=2. Motion-probing gradients were applied in three orthogonal orientations. ADC maps were automatically constructed on a pixel-by-pixel basis (0, 800 and 2,000 s/mm^2). The time required to acquire the DWI set was 5 minutes and 6 seconds.

Image analysis. All images were retrospectively analyzed by consensus by two radiologists, each with 16 years of experience, who were unaware of the clinical findings. The two readers did know that all patients in the study had biopsy-proven prostate cancer.

The readers first reviewed the axial DWI images obtained for each case using a b-value of 2000 s/mm^2, in order to identify areas suspicious for cancer. An area with focal high-SI relative to that of the surrounding prostate tissue was regarded as a cancerous lesion by consensus of the two readers. These images were reviewed in conjunction with the axial T1-weighted images and axial and coronal T2-weighted images to localize hemorrhage. An area with normal SI on DWI was regarded as non-cancerous prostate tissue. An area with diffuse high-SI in the peripheral zone on DWI was also regarded as non-cancerous tissue, since that area might be affected by hormonal therapy. The ADC values of the cancerous lesions and non-cancerous prostate tissue were measured by placement of regions of interest (ROIs). When the ROIs were drawn, great care was taken to exclude both the neurovascular bundle and the urethra. ROIs of cancerous lesions were drawn on ADC maps to include as much of the lesions as possible with the use of T2-weighted images to assist in the identification of the detailed anatomy of the prostate. ADC values of the lesions were assessed twice in the same site, and the average ADC value was calculated. For non-cancerous prostate tissue of the peripheral zone and transition zone, ROI circles were drawn in three different areas, and the ADC values were averaged.

Table I. *Characteristics of included patients.*

Characteristic	Value*
Age (years)	
Median	72
Range	55-81
Prostate-specific antigen level (ng/ml)**	
Mean	0.66
Range	0.01-10.31
Gleason score	
5	3
6	12
7	18
8	4
9	7

*Unless otherwise indicated, data represent the number of patients. **Before radiation therapy.

After radiation therapy, ADC values were measured for the cancerous lesions and non-cancerous prostate tissue. The ROI was drawn as much as possible in the same area that was initially used in the pre-radiotherapy images.

Statistical analysis. Statistical analysis was performed using the SPSS software (version 19.0J; SPSS Chicago, IL, USA). To compare the ADC values and PSA levels in patients with high SI on DWI and in patients with normal SI, the non-parametric Mann-Whitney test was used. The non-parametric Kruskal–Wallis test was used to compare the PSA levels in patients stratified by duration of hormonal therapy. The Wilcoxon signed rank test was used to compare the ADC values and PSA levels measured before and after radiation therapy. A correlation in the degree of change between serum PSA levels and ADC values was performed by use of the Pearson's correlation. A p-value of <0.05 was considered statistically significant.

Results

In 14 out of 44 patients, an area with high SI on DWI was detected (Figure 1). In these 14 patients, ten were at high risk and four were at intermediate risk for prostate cancer. The cancerous lesion was mainly detected within the peripheral zone in nine patients and in the transitional zone in five.

The mean ADC value of cancerous lesions was 0.76×10^{-3} mm^2/s, significantly smaller than that in non-cancerous prostate tissue ($1.07\times^{-3}$ mm^2/s) ($p<0.001$) (Figure 2a).

The mean PSA level in patients with high SI on DWI before radiation therapy was 1.88 ng/ml, significantly higher than that (0.08 ng/ml) in patients with normal SI on DWI ($p<0.001$) (Figure 2b).

The time from start of hormonal therapy to radiation therapy was within six months in 19 patients, six months to two years in 18, and more than two years in 7 patients. Mean PSA levels in the stratified patients were 1.07, 0.18 and 0.76 ng/ml respectively, and statistically significant differences were found ($p=0.001$).

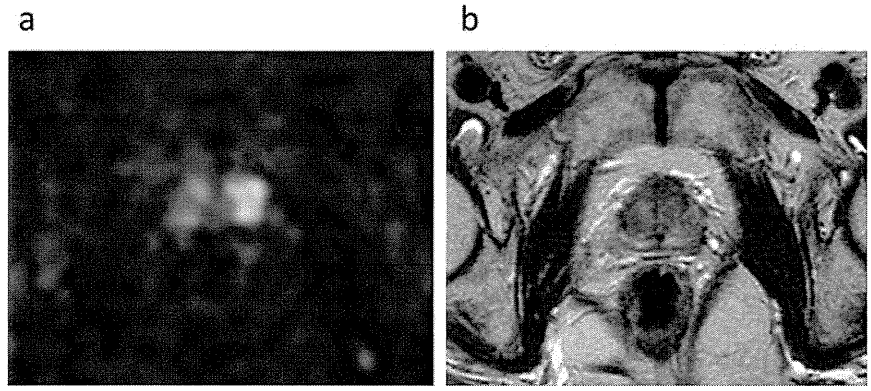

Figure 1. *A 74-year-old man with prostate cancer in the left peripheral zone. Prostate-specific antigen was 1.63 ng/ml before radiation therapy (160 ng/ml before all therapy) and the Gleason score was 8. T2-weighted image shows focal low-signal intensity in the left peripheral zone of the apex (a), and diffusion-weighted image shows focal high-signal intensity in the same region (b). The apparent diffusion co-efficient value of the lesion was* 0.642×10^{-3} *mm²/s.*

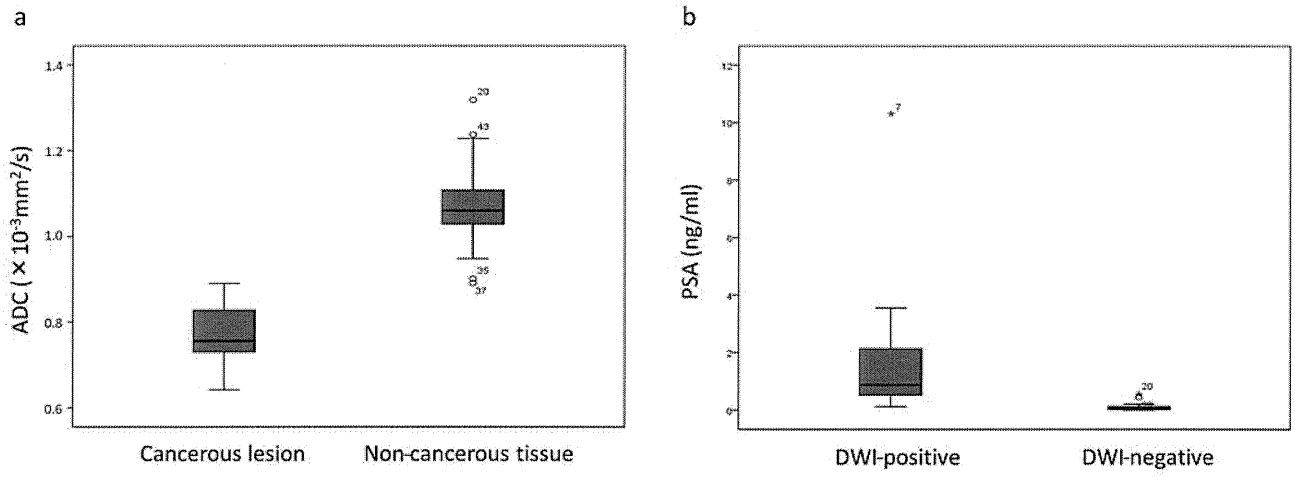

Figure 2. *Box and whisker plots illustrate the apparent diffusion co-efficient values (a) and prostate-specific antigen levels (b) in patients with high-signal lesion (the cancerous lesion) and normal signal (non-cancerous prostate tissue) on diffusion-weighted image. In this plot the horizontal lines outside each box indicate the minimum and maximum values, the box represent the value from the lower to upper quartile and is crossed by a line at the median value. Outliers are shown as dots.*

After radiation therapy, the mean ADC value of cancerous lesions increased significantly (1.02×10^{-3} mm²/s) (p=0.001) (Figure 3) and high-DWI SI disappeared. However, significant differences in the ADC values between cancerous lesions and non-cancerous tissue (1.14×10^{-3} mm²/s) remained. The mean ADC value of non-cancerous prostate tissue was statistically higher after radiation therapy (p<0.001), but the increase in the ratio was lower than in cancerous lesions.

After radiation therapy, the mean PSA level in patients with a high SI on DWI decreased significantly (0.2 ng/ml, p=0.002). The mean PSA level in patients with normal DWI signal did not change.

No correlation in the degree of changes between the PSA levels and ADC values was found (p>0.05).

Discussion

Several studies have shown that the ADC values of prostate cancer are lower than these of benign non-cancerous tissue (2-6), and, following treatment, tumor ADC values increase (7-10). This reflects increased water mobility through the loss of membrane integrity or an increase in the proportion of total extracellular fluid due to a decrease in cell size or number (12, 13).

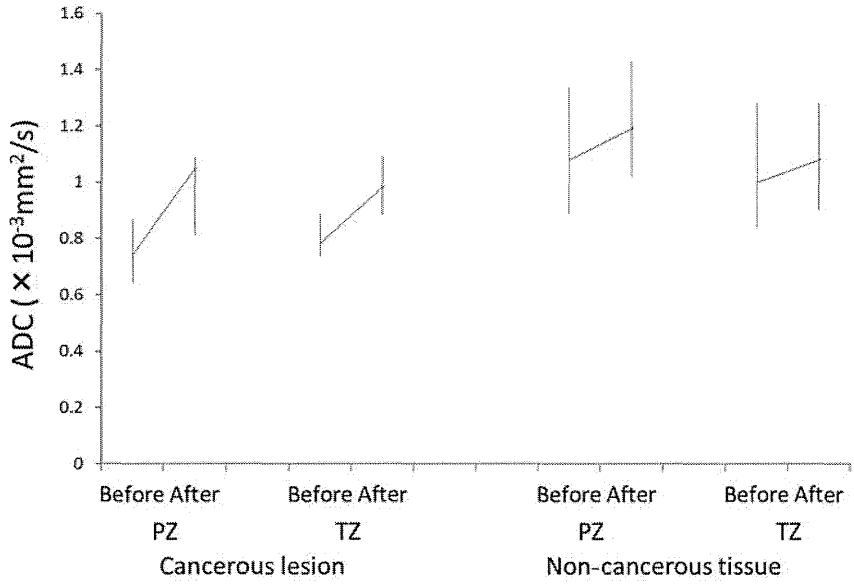

Figure 3. *Apparent diffusion co-efficient values of cancerous lesions and non-cancerous tissue before and after radiation therapy. ADC values of both cancerous lesions and non-cancerous tissue increased after radiation therapy, but the increase in the ratio of non-cancerous tissue was lower than that of cancerous lesions. PZ, Peripheral zone; TZ, transitional zone.*

The treatment effect of hormonal therapy for prostate cancer is usually evaluated with serum PSA. Imaging methods including MRI are not commonly used to monitor the treatment response in patients with prostate cancer because the measurement of PSA kinetics is simpler and more convenient. Nemoto *et al.* (10) reported that ADC values of prostate cancer increase after hormonal therapy.

In the present study, more than a quarter of the patients had areas with high SI on DWI that were regarded as cancerous lesions, despite hormonal therapy. In these patients, serum PSA levels were significantly higher than in patients with a normal DWI signal. This suggests that cancer viability remained in patients with high SI on DWI. ADC values increased significantly after radiation therapy in these patients, as has been seen in previous reports (7, 8). Thus, DWI could be used as an imaging biomarker to assess the therapeutic effect in patients with prostate cancer treated with hormonal and radiation therapy. Furthermore, as has been shown in previous reports (14-16), DWI might be used for predicting locally-recurrent prostate cancer after therapy.

The present results showed that the ADC values of non-cancerous prostate tissue also statistically increased after radiation therapy. As all patients received hormonal therapy prior to radiation therapy in the present study, the effect of hormonal therapy might remain during radiation therapy. These changes in ADC values might reflect the weakened hormonal therapy effect, especially in the peripheral zone. Several patients had an area with diffuse high-SI in the peripheral zone with relatively decreased volume and SI on T2-weighted images. These areas were excluded as cancerous lesions in order to avoid the hormonal therapy effect on normal tissue. In previous reports (17-19), histological findings in the prostate gland after hormonal therapy revealed marked glandular shrinkage, glandular atrophy, and fibrosis. These changes would be been expected to result in a smaller, darker prostate gland with relatively decreased ADC values before radiation therapy. Further investigation is needed for evaluating such ADC changes.

In the present study, all patients were treated with the same hormonal therapy but the different time from starting hormonal therapy to radiation therapy. The mean PSA levels were significantly higher in patients treated with hormonal therapy within six months or more than two years before radiotherapy. Possible reasons for this phenomenon include the following: the therapeutic effect of hormonal therapy may be inadequate when treated within six months, and PSA failure may arise when patients are treated for more than two years.

There are several limitations to this study. Firstly, no histopathological confirmation was obtained. Second, a *b* value of 2,000 s/mm^2 was used for DWI in spite of the fact that most previous reports have used a *b* value of 1,000 s/mm^2 for DWI, as is commonly used for other organs. Therefore, ADC values in the present study were relatively low compared with these of other studies; however, recent studies (20, 21) have shown that using a high *b* value of 2,000 s/mm^2 can

improve diagnostic performance in prostate cancer detection.

In conclusion, the present results suggest that SI on DWI appears to correlate with PSA levels for prostate cancer treated with radiation and hormonal therapy. ADC values appear to be useful for monitoring the therapeutic response of prostate cancer.

References

1 Fitzpatrick JM, Bnau E and Oudard S: Prostate-specific antigen kinetics in localized and advanced prostate cancer. BJU Int *103*: 578-587, 2009.

2 Haider MA, van der Kwast TH, Tanguay J, Evans AJ, Hashmi AT, Lockwood G and Trachtenberg J: Combined T2-weighted and diffusion-weighted MRI for localization of prostate cancer. Am J Roentgenol *189*: 323-328, 2007.

3 Weinreb JC, Blume JD, Coakley FV, Wheeler TM, Cormack JB, Sotto CK, Cho H, Kawashima A, Tempany-Afdhal CM, Macura KJ, Rosen M, Gerst SR and Kurhanewicz J: Prostate cancer: Sextant localization at MR imaging and MR spectroscopic imaging before prostatectomy–results of ACRIN prospective multi-institutional clinicopathologic study. Radiology *251*: 122-133, 2009.

4 Rosenkrantz AB, Kong X, Niver BE, Berkman DS, Melamed J, Babb JS and Taneja SS: Prostate cancer: Comparison of tumour visibility on trace diffusion-weighted images and the apparent diffusion coefficient map. Am J Roentgenol *196*: 123-129, 2011.

5 Rosenkrantz AB, Mannelli L, Kong X, Niver BE, Berkman DS, Babb JS, Melamed J and Taneja SS: Prostate cancer: Utility of fusion of T2-weighted and high b-value diffusion-weighted images for peripheral zone tumour detection and localization. J Magn Reson Imaging *34*: 95-100, 2011.

6 Kim CK, Park BK, Han JJ, Kang TW and Lee HM: Diffusion-weighted imaging of the prostate at 3 T for differentiation of malignant and benign tissue in transition and peripheral zones: Preliminary results. J Comput Assist Tomogr *31*: 449-454, 2007.

7 Takayama Y, Kishimoto R, Hanaoka S, Nonaka H, Kandatsu S, Tsuji H, Tsujii H, Ikehira H and Obata T: ADC value and diffusion tensor imaging of prostate cancer: Changes in carbon-ion radiotherapy. J Magn Reson Imaging *27*: 1331-1335, 2008.

8 Song I, Kim CK, Park BK and Park W: Assessment of response to radiotherapy for prostate cancer: Value of diffusion-weighted MRI at 3 T. Am J Roentgenol *194*: 477-482, 2010.

9 De Visschere PJ, De Meerleer GO, Futterer JJ and Villeirs GM: Role of MRI in follow-up after focal therapy for prostate carcinoma. Am J Roentgenol *194*: 1427-1433, 2010.

10 Nemoto K, Tateishi T and Ishida T: Changes in diffusion-weighted images for visualizing prostate cancer during antiandrogen therapy: Preliminary results. Urol Int *85*: 421-426, 2010.

11 D'Amico AV, Cote K, Loffredo M, Renshaw AA and Schultz D: Determinants of prostate cancer-specific survival following radiation therapy during the prostate-specific antigen era. J Urol *170*: S42-47, 2003.

12 Padhani AR, Liu G, Koh DM, Chenevert TL, Thoeny HC, Takahara T, Dzik-Jurasz A, Ross BD, Van Cauteren M, Collins D, Hammoud DA, Rustin GJ, Taouli B and Choyke PL: Diffusion-weighted magnetic resonance imaging as a cancer biomarker: Consensus and recommendations. Neoplasia *11*: 102-125, 2009.

13 Hamstra DA, Rehemtulla A and Ross BD: Diffusion magnetic resonance imaging: A biomarker for treatment response in oncology. J Clin Oncol *25*: 4104-4109, 2007.

14 Kim CK, Park BK and Lee HM: Prediction of locally recurrent prostate cancer after radiation therapy: Incremental value of 3T diffusion-weighted MRI. J Magn Reson Imaging *29*: 391-397, 2009.

15 Kim CK, Park BK and Lee HM: MRI techniques for prediction of local tumour progression after high-intensity focused ultrasonic ablation of prostate cancer. Am J Roentgenol *190*: 1180-1186, 2008.

16 Akin O, Gultekin DH, Vargas HA, Zheng J, Moskowitz C, Pei X, Sperling D, Schwartz LH, Hricak H and Zelefsky MJ: Incremental value of diffusion weighted and dynamic contrast enhanced MRI in the detection of locally recurrent prostate cancer after radiation treatment: Preliminary results. Eur Radiol *21*: 1970-1978, 2011.

17 Murphy WM, Soloway MS and Barrows GH: Pathologic changes associated with androgen deprivation therapy for prostate cancer. Cancer *68*: 821-828, 1991.

18 Smith DM and Murphy WM: Histologic changes in prostate carcinomas treated with leuprolide (luteinizing hormone-releasing hormone effect): Distinction from poor tumour differentiation. Cancer *73*: 1472-1477, 1994.

19 Padhani AR, MacVicar AD, Gapinski CJ, earnaley DP, Parker GJ, Suckling J, Leach MO and Husband JE: Effects of androgen deprivation on prostatic morphology and vascular permeability evaluated with MR imaging. Radiology *218*: 365-374, 2001.

20 Katahira K, Takahara T, Kwee TC, Oda S, Suzuki Y, Morishita S, Kitani K, Hamada Y, Kitaoka M and Yamashita Y: Ultra-high -b-value diffusion-weighted MR imaging for the detection of prostate cancer: Evaluation in 201 cases with histopathological correlation. Eur Radiol *1*: 188-196, 2011.

21 Kitajima K, Kaji Y, Kuroda K and Sugimura K: High b-value diffusion-weighted imaging in normal and malignant peripheral zone tissue of the prostate: Effect of signal-to noise ratio. Magn Reson Med Sci *7*: 93-99, 2008.

Received June 29, 2012
Revised August 8, 2012
Accepted August 9, 2012

Journal of Radiation Research, 2013, 54, 113–125
doi: 10.1093/jrr/rrs083 Advance Access Publication 17 September 2012

Analysis of late toxicity associated with external beam radiation therapy for prostate cancer with uniform setting of classical 4-field 70 Gy in 35 fractions: a survey study by the Osaka Urological Tumor Radiotherapy Study Group

Yasuo YOSHIOKA[1,*], Osamu SUZUKI[2], Kazuo NISHIMURA[3], Hitoshi INOUE[4], Tsuneo HARA[4], Ken YOSHIDA[5], Atsushi IMAI[6], Akira TSUJIMURA[7], Norio NONOMURA[7] and Kazuhiko OGAWA[1]

[1]Department of Radiation Oncology, Osaka University Graduate School of Medicine, 2-2 Yamadaoka, Suita, Osaka 565-0871, Japan
[2]Department of Radiation Oncology, Osaka Medical Center for Cancer and Cardiovascular Diseases, 1-3-3 Nakamichi, Higashinari-ku, Osaka 537-8511, Japan
[3]Department of Urology, Osaka Medical Center for Cancer and Cardiovascular Diseases, 1-3-3 Nakamichi, Higashinari-ku, Osaka 537-8511, Japan
[4]Department of Urology, Ikeda City Hospital, 3-1-18 Jonan, Ikeda, Osaka 563-8510, Japan
[5]Department of Radiation Oncology and Institute for Clinical Research, National Hospital Organization Osaka National Hospital, 2-1-14 Hoenzaka, Chuo-ku, Osaka 540-0006, Japan
[6]Department of Radiation Oncology, Sumitomo Hospital, 5-3-20 Nakanoshima, Kita-ku, Osaka 530-0005, Japan
[7]Department of Urology, Osaka University Graduate School of Medicine, 2-2 Yamadaoka, Suita, Osaka 565-0871, Japan
*Corresponding author. Tel: +81-6-6879-3482; Fax: +81-6-6879-3489; Email: yoshioka@radonc.med.osaka-u.ac.jp

(Received 26 April 2012; revised 15 August 2012; accepted 16 August 2012)

We aimed to analyse late toxicity associated with external beam radiation therapy (EBRT) for prostate cancer using uniform dose-fractionation and beam arrangement, with the focus on the effect of 3D (CT) simulation and portal field size. We collected data concerning patients with localized prostate adenocarcinoma who had been treated with EBRT at five institutions in Osaka, Japan, between 1998 and 2006. All had been treated with 70 Gy in 35 fractions, using the classical 4-field technique with gantry angles of 0°, 90°, 180° and 270°. Late toxicity was evaluated strictly in terms of the Common Terminology Criteria for Adverse Events Version 4.0. In total, 362 patients were analysed, with a median follow-up of 4.5 years (range 1.0–11.6). The 5-year overall and cause-specific survival rates were 93% and 96%, respectively. The mean ± SD portal field size in the right–left, superior–inferior, and anterior–posterior directions was, respectively, 10.8 ± 1.1, 10.2 ± 1.0 and 8.8 ± 0.9 cm for 2D simulation, and 8.4 ± 1.2, 8.2 ± 1.0 and 7.7 ± 1.0 cm for 3D simulation ($P < 0.001$). No Grade 4 or 5 late toxicity was observed. The actuarial 5-year Grade 2–3 genitourinary and gastrointestinal (GI) late toxicity rates were 6% and 14%, respectively, while the corresponding late rectal bleeding rate was 23% for 2D simulation and 7% for 3D simulation ($P < 0.001$). With a uniform setting of classical 4-field 70 Gy/35 fractions, the use of CT simulation and the resultant reduction in portal field size were significantly associated with reduced late GI toxicity, especially with less rectal bleeding.

Keywords: prostate cancer; late toxicity; portal field size; CT simulation; external beam radiation therapy

INTRODUCTION

Since radiotherapy for prostate cancer is a standard treatment option for localized prostate cancer, its toxicity should be clearly addressed. In a previous survey study conducted from 1995 to 2006 in Osaka, Japan, which was intended to clarify time trends in radiotherapy and its biochemical relapse-free survival (bRFS) outcomes, we made the interesting discovery that 87% of patients had been treated with a highly uniform mode of radiotherapy, that is,

with classical 4-field 70 Gy in 35 fractions [1]. While that study was being conducted, CT simulation was introduced and developed, and almost all institutions had replaced 2D simulation with 3D simulation by 2006. This resulted in a reduction in the size of the portal field. We realized that we could obtain very pure data for an investigation of the relationship between portal field size and late toxicity rate, especially for rectal bleeding, in view of the uniform setting of dose-fractionation and beam arrangement. The findings of this investigation are the main subject of this article. Dearnaley *et al.* had already conducted a prospective randomized trial comparing 1.0 and 1.5 cm margins, and concluded that a larger margin was associated with significantly higher incidence of toxicities [2]. However, their study included only 126 patients, who had been assigned to 2×2 arms (64 Gy and 74 Gy groups, and 1.0 and 1.5 cm margin groups). Moreover, their treatment planning included two phases comprising a 3-field phase and a 6-field phase. We aimed to repeat the investigation with a larger Japanese patient cohort, treated with more uniform dose-fractionation and beam arrangement, although in a retrospective manner.

MATERIALS AND METHODS

A brief summary of the previous survey study

In our previous study [1], data were collected for 652 consecutive patients with clinically localized prostate cancer (T1-4N0M0), who had been treated with definitive external beam radiotherapy (EBRT) of 60 Gy or more at one of the 11 participating institutions, mainly in Osaka, Japan, from 1995 through 2006. Of the 652 patients, 436 met the enrolment criteria and were analysed. The main findings were: (i) the number of radiotherapy patients showed a 10-fold increase over 10 years; (ii) the dominant dose-fractionation was 70 Gy/35 fractions (87%); (iii) hormone therapy had been administered to 95% of the patients; (iv) the 3- and 5-year bRFS rates were 85% and 70%, respectively; (v) toxicity data was not available.

An interesting finding was that as many as 87% of the patients had received radiotherapy in a highly uniform manner, that is, with the classical 4-field technique using a dose-fractionation schedule of 70 Gy/35 fractions. We therefore planned the second survey by focusing on detailed late toxicity data and irradiation field data obtained with a uniform setting of 4-field 70 Gy/35 fractions.

Data collection

Five institutions participated in the present study. Data collected for the 362 patients who are the subject of this study are described in the Results section.

All the data were collected by physicians (radiation oncologists or urologists), who are also the authors of this paper, and no non-physician surveyors took any part in this study. Detailed information was collected about portal field size and other parameters of radiotherapy. Late toxicity grading was performed by retrospectively reviewing medical charts, strictly according to the Common Terminology Criteria for Adverse Events (CTCAE) Version 4.0. The concrete description of each relevant CTCAE Term was gathered as Tables 1 and 2, which had been distributed to the surveyors as references. All data were sent to Osaka University, analysed by the first author, and finally reviewed and approved by all the authors.

Statistical Analysis

The unpaired t test was used to compare the averages of the two groups, while Fisher's exact test was used to compare the proportions. Kaplan-Meier curves were obtained for survival and toxicity rates, and the log-rank test was used to compare them. A P-value <0.05 was deemed statistically significant. Statistical analysis was performed with PASW Statistics 18 software (SPSS, Inc., Chicago, IL, USA).

RESULTS

Data for a total of 362 patients, all of whom had been treated for T1-4N0M0 adenocarcinoma of the prostate between 1998 and 2006, were collected from five representative institutions in Osaka, Japan. Postoperative cases were not included. None of the patients had been irradiated to the elective lymph node region, and all had been treated with the classical 4-field technique using 70 Gy in 35 fractions with gantry angles of 0°, 90°, 180° and 270°.

The median and mean ages of the patients were both 70 years (range, 49–82). The median follow-up period was 4.5 years (range, 1.0–11.6), with a minimum of 1 year. The actuarial 5-year overall and prostate cancer-specific survival rates were 93% and 96%, respectively (Fig. 1).

Neoadjuvant hormone therapy had been administered to 328 patients (91%), 35 of whom (11 %) had been considered hormone-refractory at the time of radiotherapy. Adjuvant hormone therapy had been administered to 276 of the total of 362 patients (76%), and 179 of them (65%) had already discontinued the therapy at the time of this survey. The median durations of neoadjuvant and adjuvant hormone therapy were 8 months (range, 1–150) and 24 months (range, 1–129), respectively.

2D simulation was performed for 127 patients, all of whom had been treated between 1998 and 2003. The other 235 had been treated using 3D simulation with a CT-simulator between 1998 and 2006. Of the five institutions, three had a 1 cm-width multileaf collimator (MLC), one a 2-cm MLC and one a 1-cm MLC until 2006, which was then replaced with a 0.5-cm MLC. The energy of the anterior-posterior beam was 10 MV at four institutions, and 20 MV at one. The energy of the lateral beams was 10 MV at three institutions, and 18 MV and 20 MV at one each. A

Table 1. Late genitourinary toxicity scale extracted from the Common Terminology Criteria for Adverse Events (CTCAE) Version 4.0

Renal and urinary disorders					
	Grade				
Adverse Event	**1**	**2**	**3**	**4**	**5**
Hematuria	Asymptomatic; clinical or diagnostic observations only; intervention not indicated	Symptomatic; urinary catheter or bladder irrigation indicated; limiting instrumental ADL	Gross hematuria; transfusion, IV medications or hospitalization indicated; elective endoscopic, radiologic or operative intervention indicated; limiting self care ADL	Life-threatening consequences; urgent radiologic or operative intervention indicated	Death
Definition: A disorder characterized by laboratory test results that indicate blood in the urine.					
Urinary frequency	Present	Limiting instrumental ADL; medical management indicated	–	–	–
Definition: A disorder characterized by urination at short intervals.					
Urinary incontinence	Occasional (e.g. with coughing, sneezing, etc.), pads not indicated	Spontaneous; pads indicated; limiting instrumental ADL	Intervention indicated (e.g. clamp, collagen injections); operative intervention indicated; limiting self care ADL	–	–
Definition: A disorder characterized by inability to control the flow of urine from the bladder.					
Urinary retention	Urinary, suprapubic or intermittent catheter placement not indicated; able to void with some residual	Placement of urinary, suprapubic or intermittent catheter placement indicated; medication indicated	Elective operative or radiologic intervention indicated; substantial loss of affected kidney function or mass	Life-threatening consequences; organ failure; urgent operative intervention indicated	Death
Definition: A disorder characterized by accumulation of urine within the bladder because of the inability to urinate.					
Urinary tract obstruction	Asymptomatic; clinical or diagnostic observations only	Symptomatic but no hydronephrosis, sepsis or renal dysfunction; urethral dilation, urinary or suprapubic catheter indicated	Symptomatic and altered organ function (e.g. hydronephrosis, or renal dysfunction); elective radiologic, endoscopic or operative intervention indicated	Life-threatening consequences; urgent intervention indicated	Death

Continued

Table 1. *Continued*

Renal and urinary disorders					
	Grade				
Adverse Event	**1**	**2**	**3**	**4**	**5**
Definition: A disorder characterized by blockage of the normal flow of contents of the urinary tract.					
Urinary tract pain	Mild pain	Moderate pain; limiting instrumental ADL	Severe pain; limiting self care ADL	–	–
Definition: A disorder characterized by a sensation of marked discomfort in the urinary tract.					
Urinary urgency	Present	Limiting instrumental ADL; medical management indicated	–	–	–
Definition: A disorder characterized by a sudden compelling urge to urinate.					
Urine discoloration	Present	–	–	–	–
Definition: A disorder characterized by a change in the color of the urine.					
Renal and urinary disorders - Other, specify	Asymptomatic or mild symptoms; clinical or diagnostic observations only; intervention not indicated	Moderate, local or noninvasive intervention indicated; limiting instrumental ADL	Severe or medically significant but not immediately life-threatening; hospitalization or prolongation of existing hospitalization indicated; disabling; limiting self care ADL	Life-threatening consequences; urgent intervention indicated	Death

Table 2. Late gastrointestinal toxicity scale extracted from the Common Terminology Criteria for Adverse Events (CTCAE) Version 4.0

Gastrointestinal disorders					
	Grade				
Adverse Event	**1**	**2**	**3**	**4**	**5**
Abdominal pain	Mild pain	Moderate pain; limiting instrumental ADL	Severe pain; limiting self care ADL	–	–
Definition: A disorder characterized by a sensation of marked discomfort in the abdominal region.					
Anal fistula	Asymptomatic; clinical or diagnostic observations only; intervention not indicated	Symptomatic; altered GI function	Severely altered GI function; tube feeding, TPN or hospitalization indicated; elective operative intervention indicated	Life-threatening consequences; urgent intervention indicated	Death
Definition: A disorder characterized by an abnormal communication between the opening in the anal canal to the perianal skin.					
Anal hemorrhage	Mild; intervention not indicated	Moderate symptoms; medical intervention or minor cauterization indicated	Transfusion, radiologic, endoscopic, or elective operative intervention indicated	Life-threatening consequences; urgent intervention indicated	Death
Definition: A disorder characterized by bleeding from the anal region.					
Anal mucositis	Asymptomatic or mild symptoms; intervention not indicated	Symptomatic; medical intervention indicated; limiting instrumental ADL	Severe symptoms; limiting self care ADL	Life-threatening consequences; urgent intervention indicated	Death
Definition: A disorder characterized by inflammation of the mucous membrane of the anus.					
Anal necrosis	–	–	TPN or hospitalization indicated; radiologic, endoscopic, or operative intervention indicated	Life-threatening consequences; urgent operative intervention indicated	Death
Definition: A disorder characterized by necrotic process occurring in the anal region.					
Anal pain	Mild pain	Moderate pain; limiting instrumental ADL	Severe pain; limiting self care ADL	–	–
Definition; A disorder characterized by a sensation of marked discomfort in the anal region.					
Anal stenosis	Asymptomatic; clinical or diagnostic observations only; intervention not indicated	Symptomatic; altered GI function	Symptomatic and severely altered GI function; non-emergent operative intervention	Life-threatening consequences; urgent operative intervention indicated	Death

Continued

Table 2. *Continued*

Gastrointestinal disorders					
	Grade				
Adverse Event	**1**	**2**	**3**	**4**	**5**
			indicated; TPN or hospitalization indicated		
Definition: A disorder characterized by a narrowing of the lumen of the anal canal.					
Anal ulcer	Asymptomatic; clinical or diagnostic observations only; intervention not indicated	Symptomatic; altered GI function	Severely altered GI function; TPN indicated; elective operative or endoscopic intervention indicated; disabling	Life-threatening consequences; urgent operative intervention indicated	Death
Definition: A disorder characterized by a circumscribed, inflammatory and necrotic erosive lesion on the mucosal surface of the anal canal.					
Constipation	Occasional or intermittent symptoms; occasional use of stool softeners, laxatives, dietary modification, or enema	Persistent symptoms with regular use of laxatives or enemas; limiting instrumental ADL	Obstipation with manual evacuation indicated; limiting self care ADL	Life-threatening consequences; urgent intervention indicated	Death
Definition: A disorder characterized by irregular and infrequent or difficult evacuation of the bowels.					
Diarrhea	Increase of <4 stools per day over baseline; mild increase in ostomy output compared to baseline	Increase of 4-6 stools per day over baseline; moderate increase in ostomy output compared to baseline	Increase of ≥7 stools per day over baseline; incontinence; hospitalization indicated; severe increase in ostomy output compared to baseline; limiting self care ADL	Life-threatening consequences; urgent intervention indicated	Death
Definition: A disorder characterized by frequent and watery bowel movements.					
Fecal incontinence	Occasional use of pads required	Daily use of pads required	Severe symptoms; elective operative intervention indicated	–	–
Definition: A disorder characterized by inability to control the escape of stool from the rectum.					
Hemorrhoidal hemorrhage	Mild; intervention not indicated	Moderate symptoms; medical intervention or minor cauterization indicated	Transfusion, radiologic, endoscopic, or elective operative intervention indicated	Life-threatening consequences; urgent intervention indicated	Death

Definition: A disorder characterized by bleeding from the hemorrhoids.					
Hemorrhoids	Asymptomatic; clinical or diagnostic observations only; intervention not indicated	Symptomatic; banding or medical intervention indicated	Severe symptoms; radiologic, endoscopic or elective operative intervention indicated	–	–
Definition: A disorder characterized by the presence of dilated veins in the rectum and surrounding area.					
Ileus	–	Symptomatic; altered GI function; bowel rest indicated	Severely altered GI function; TPN indicated	Life-threatening consequences; urgent intervention indicated	Death
Definition: A disorder characterized by failure of the ileum to transport intestinal contents.					
Proctitis	Rectal discomfort, intervention not indicated	Symptoms (e.g. rectal discomfort, passing blood or mucus); medical intervention indicated; limiting instrumental ADL	Severe symptoms; fecal urgency or stool incontinence; limiting self care ADL	Life-threatening consequences; urgent intervention indicated	Death
Definition: A disorder characterized by inflammation of the rectum.					
Rectal fistula	Asymptomatic; clinical or diagnostic observations only; intervention not indicated	Symptomatic; altered GI function	Severely altered GI function; TPN or hospitalization indicated; elective operative intervention indicated	Life-threatening consequences; urgent intervention indicated	Death
Definition: A disorder characterized by an abnormal communication between the rectum and another organ or anatomic site.					
Rectal hemorrhage	Mild; intervention not indicated	Moderate symptoms; medical intervention or minor cauterization indicated	Transfusion, radiologic, endoscopic or elective operative intervention indicated	Life-threatening consequences; urgent intervention indicated	Death
Definition: A disorder characterized by bleeding from the rectal wall and discharge from the anus.					
Rectal mucositis	Asymptomatic or mild symptoms; intervention not indicated	Symptomatic; medical intervention indicated; limiting instrumental ADL	Severe symptoms; limiting self care ADL	Life-threatening consequences; urgent operative intervention indicated	Death
Definition: A disorder characterized by inflammation of the mucous membrane of the rectum.					
Rectal necrosis	–	–	Tube feeding or TPN indicated; radiologic, endoscopic, or operative intervention indicated	Life-threatening consequences; urgent operative intervention indicated	Death
Definition: A disorder characterized by a necrotic process occurring in the rectal wall.					
Rectal obstruction	Asymptomatic; clinical or	Symptomatic; altered GI	Hospitalization indicated;	Life-threatening consequences;	Death

Continued